

# Optimal Design of Steppers in Single Step High Pressure Torsion (SIHPT) Process as a Novel SPD Method

**Mehdi Eskandarzade**

Department of Mechanical Engineering,  
University of Mohaghegh Ardabili, Iran  
E-mail: m.eskandarzade@gmail.com

**Ghader Faraji\*, Abolfazl Masoumi**

Department of Mechanical Engineering,  
University of Tehran, Iran  
E-mail: ghfaraji@ut.ac.ir\*, amasomi@ut.ac.ir

\*Corresponding author

**Ali Kalaki**

Department of Technical and Corrosion Protection,  
Iranian Central Oil Fields Company, Iran  
E-mail: alikalaki@yahoo.com

**Received: 29 January 2018, Revised: 3 April 2018, Accepted: 10 August 2018**

**Abstract:** Single Step High Pressure Torsion (SIHPT) is a newly developed HPT based method for processing of materials which is capable of producing nanostructured long samples with characteristics comparable to conventional HPT process. While, conventional HPT can be applied only on thin samples; it is possible to produce nanostructured parts with about 10 cm long using SIHPT method. However, SIHPT needs some technical improvements in order to be used for production in an industrial scale. One of the key component of SIHPT is the steppers which help different sections of the sample to be twisted. This study investigates the main parameters of steppers including the corner radius, thickness and rotation speed. The experimental results revealed that for the lowest length of sample's contact inside the steppers (lower contact length) of 5mm; there is considerable slippage in pressures below 1GP. However, the amount of slippage decreases gradually by increasing the magnitude of the applied pressure and the amount of the lower contact length. Moreover, it was found that the rotational speed influences the amount of slippage in low pressures (lower than 1 GPa) but not in high pressures. In addition, according to Finite Element (FE) analysis it was found that 1 mm corner radius of steppers is the optimal value for the SIHPT process.

**Keywords:** Friction, Single Step Incremental High Pressure Torsion (SIHPT), Slippage

**Reference:** Eskandarzade, M., Faraji, G., Masoumi, A., and Kalaki, A., "Optimal Design of Steppers in Single Step High Pressure Torsion (SIHPT) Process as a Novel SPD Method", Int J of Advanced Design and Manufacturing Technology, Vol. 12/No. 1, 2019, pp. 41–50.

**Biographical notes:** **Mehdi Eskandarzade** is Assistant Professor at Mohaghegh Ardabili, Ardabil University, Iran. His current research interest includes Corrosion in Oil and Gas Industry. **Ghader Faraji** is Associate Professor at Tehran University, Iran. His current research focuses on Nanostructure Materials, SPD Methods. **Abolfazl Masoumi** is Full Professor at Tehran University, Iran. His current research focuses on Computer Aided Manufacturing and Metal Forming. **Ali Kalaki** is head of Technical and Corrosion Protection Department, Iranian Central Oil Fields Company, Iran.

## 1 INTRODUCTION

High pressure torsion (HPT) process is a type of severe plastic deformation method for the production of nanostructured parts. HPT produced copper samples normally have an average grain size of about 300nm or less. In a conventional HPT method, there is a great restriction in terms of sample's thickness and diameter. The fundamental of HPT process was first reported by Bridgman in 1935 [1]. Basic information regarding HPT process can be found in the literature [2]. It is unanimously agreed that as the strain increases, more microstructural grain refinement occurs. However, after the saturation point, the microstructure refinement is stopped despite applying more strains [3].

There are several researches dedicated to study the behavior of the materials under high hydrostatic pressure conditions using numerical methods [4-5]. The first step at HPT process is the production of very high hydrostatic pressure inside the material. The results of FEM analysis show that after the application of 8 GPa hydrostatic pressure in a copper specimen, the strain values of about two are reachable at the outside diameter of the specimen [6-7]. Application of torsion stresses followed by hydrostatic pressure will lead to greater refinement of the microstructure [8].

While some researchers [9] are employed deformable specimen and rigid die in their numerical models; Verleysen et al [10] suggested to use deformable behavior for both the specimen and die in order to achieve more accurate results. However, this kind of modelling needs huge computational memory and the task of modelling using this approach is very time consuming and difficult for most of die and samples configurations. The effect of applied pressure and the friction factor on the distribution of equivalent strains in HPT processed parts are offered in the literature [11-12]. The low speed of the HPT process is one of the great deficiencies of the HPT method.

The main reason for keeping low speed for HPT process is to eliminate the recrystallization of the refined microstructure due to the heat production by frictional forces. This issue has been discussed by Figueiredo et al. [13] using FEM analysis. According to the results, the rate of heat production is directly proportional to the mechanical strength of the specimen and the rotational speed of the die. The same work finally concludes that it is possible to raise the rotational speed without recrystallization just by utilizing bulkier anvils.

In traditional HPT process, it is common to fix one of the anvils and rotate another relatively. However, the investigation of Jahedi et al [14] revealed that it is possible to reach higher strain values by rotating both anvils in reverse directions. Another important parameter of the HPT process is the torque needs for rotation of the anvils. FEM studies show that the needed

torque for the copper specimen is dependently augmented with increasing the rotation angle up to 0.1 radians. After this value, more rotation is possible without any increment in torque value [15-16].

One of the great challenges of researchers who work on HPT process is to extend the application of the process for long specimens. There are some successful steps toward the application of HPT process to relatively long parts. Incremental High Pressure Torsion (IHPT) developed by Hohenwarter is one of these works [17]. Another important work in this regard is known as Single Step High Pressure Torsion (SIHPT) method which is developed recently by the current authors [18]. Although there are several researchers to investigate different aspects of traditional HPT process, important parameters of SIHPT process have not been studied yet. In this study, because of the great importance of the steppers in SIHPT process, design parameters of Steppers including corner radius, thickness and rotational speed are investigated numerically and experimentally.

## 2 DESIGN PARAMETERS OF THE STEPPERS IN SIHPT PROCESS

Figure 1 shows the schematic of the SIHPT process. As it is obvious, like the traditional HPT, the specimen is located inside the fixed and rotating anvils; however; anvils in the SIHPT method are composed of several thin steppers ("Fig. 2") instead of integrated part. The length of the fixed and rotating anvils can be controlled via two casings in SIHPT method ("Fig. 1"). The specimen diameter is the same with the diameter of the steppers; but the specimen length is a little larger.

This intentional overhang is necessary to have control over the real hydrostatic pressure inside a specimen. Similar to traditional HPT, the SIHPT process consists of high hydrostatic pressure on the specimen, which is followed by a rotation of sliding steppers (confined inside casing 1 in "Fig. 1") against fixed steppers (confined inside casing 2 in "Fig. 1") with a very low speed. The rotation of the steppers introduces intensive torsional stresses in a region near the interface of sliding and fixed steppers.

The length of the specimen is too long to be processed in one step. Therefore, in SIHPT process, the processing of the whole length is done by subsequent relative rotation of the steppers. It means that after the processing of a given region (near the rotation interface), the location of the strain induced region is shifted up or down by changing the number of steppers confined in fixed and rotating casings to designate another length of the specimen. The detail of the SIHPT process is elaborated in reference [17].

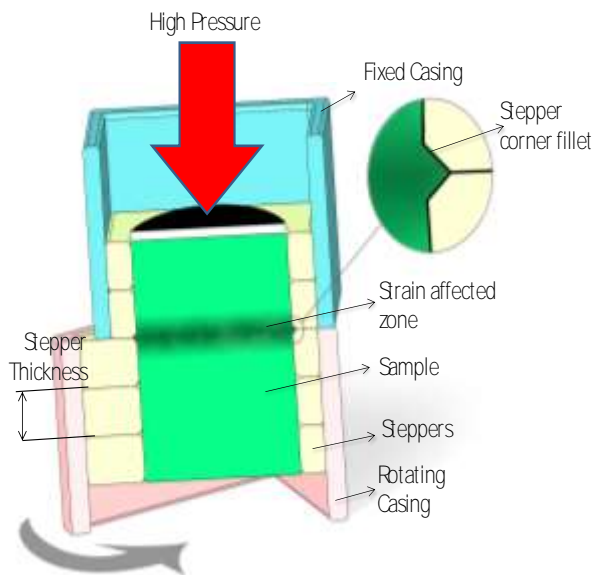


**Fig. 1** Schematic of the SIHPT cross section, casing 1 & 2 can be displaced upward and downward.



**Fig. 2** One of anvils which consists of several steppers (sample is located inside the Steppers).

In SIHPT method by squeezing a sample between two anvils and by applying a very high hydrostatic pressure, the material flows into corner radius of the steppers until the balance between the frictional forces and the applied pressure occurs. The Steppers' corner radius plays important role in stress and strain distribution through the material. The thickness of the steppers determines the amount of nanostructured region in each step and also influences the slippage phenomenon at the rotation step of the process. The other parameter which affects the amount of slippage in SIHPT method is the rotation speed. This issue will be discussed in the next sections.

### 3 SLIPPAGE IN SIHPT PROCESS

Figure 3 shows the experimental setup of this study. In

SIHPT process, in order to avoid the slippage during the rotational stage, it is very important to assure that the frictional forces between the specimen and the steppers to be enough to overcome the shear yield strength of the material. According to Amonton's friction model ("Eq. 1") the relation between the hydrostatic pressure and the frictional shear strength of the interference is as following:

$$\tau_f = \mu P_a \tag{1}$$

Where,  $P_a$  denotes hydrostatic pressure and  $\tau_f$  is the frictional shear strength of the interference and  $\mu$  is friction coefficient at high pressures and low speed conditions. The experimental procedure for measuring friction coefficient at the condition of the SPD process has been offered in the literature [19].

The shortest contact length ( $L$ ) between the specimen and the constant die is the key parameter in slippage phenomenon. This length is considered as equal as the thickness of single stepper. This is because, the most critical condition occurs where the fixed anvil consists of only one stepper. In this condition, the fixed casing confined a single stepper and the contact length is equal with the thickness of this single stepper. Neglecting the friction force between the sample tips and die, the friction force between the die and the cylindrical surface of the specimen ( $F_f$ ) can be calculated via "Eq. (2)":

$$F_f = \tau_f \times \pi dL \text{ or } F_f = \mu P_a \times \pi dL \tag{2}$$

Where  $d$  is specimen diameter.

On the other hand, the required force ( $F_r$ ) to overcome the shear yield strength ( $\tau_{sy}$ ) of the nanostructured material is calculated as "Eq. (3)":

$$F_r = \tau_{sy} \times \frac{\pi d^2}{4} \tag{3}$$

In order to do successful experiment the condition  $F_r < F_f$  should be satisfied which means:

$$L \geq \frac{\tau_{sy}}{\mu P_a} \cdot \frac{d}{4} \tag{4}$$

As it is clear from "Eq. 4", the minimum required length of contact ( $L$ ) for theoretically no slippage condition is directly dependent on the material shear yield strength ( $\tau_{sy}$ ), and has a relation with the inverse of friction coefficient ( $\mu$ ) and the magnitude of hydrostatic pressure ( $P_a$ ). Here, for the purpose of the current investigation, the slippage is defined explicitly as the difference between the measured torsional rotation of the sample and the rotation imposed externally by the processing facility.

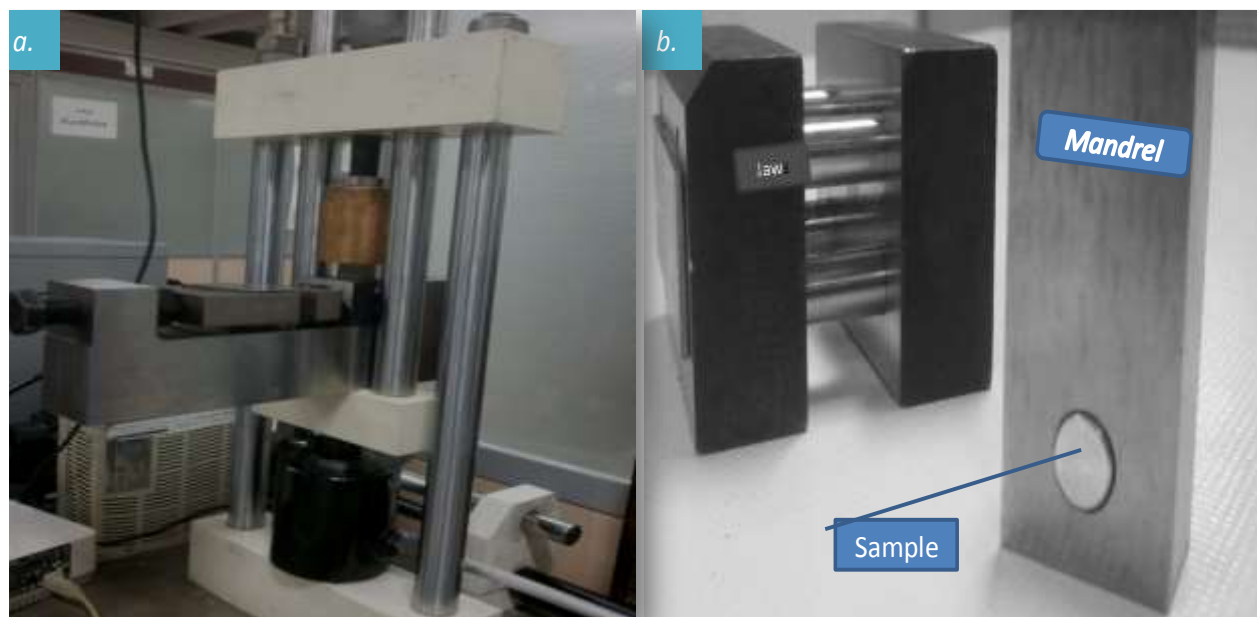


**Fig. 3** (a): Experimental setup for measuring friction coefficient and (b): Jaws and specimen inside a mandrel.

## 4 EXPERIMENTAL PROCEDURE

### 4.1. Friction Measurements

It is known that the friction coefficient between material pair changes drastically by changing in normal pressure but generally remains approximately unchanged after reaches its minimum in higher pressures [19]. Here, it needs to measure the coefficient of friction in order to use in finite element simulations. To aim this goal, in this study the friction coefficient values between copper specimen and steel die is measured for different normal pressures, experimentally. The results revealed that the friction coefficient for steel-copper pair system is about 0.22 for pressures higher than 0.8 GPa which is the case in SIHPT process. Figure 3(a) shows the experimental setup which is used in this study for friction coefficient measurements. The details of the friction coefficient measurement procedure can be found in the literature [19].

In the friction measurement experiments of this study, Jaws were made of AISI 4340 steel with hardened surfaces up to 60 Rockwell C. Specimens were made from technically pure copper samples. The tips of the specimens had the as machined surface roughness as the real experiment in SIHPT process.

### 4.2. Slippage Measurement Procedure

In this study, as shown in “Fig. 4”, in order to measure the amount of slippage, a line was scribed along the length and tips of each sample. Then, samples were

placed in SIHPT facility and they separately rotated about  $\frac{1}{4}$ ,  $\frac{1}{2}$ , 1 and 2 revolutions. Figure 5 (left) shows the sample inside of the SIHPT facility. In practice the length of the sample gets shortened after the application of pressure. Preliminary tests revealed that after the application of hydrostatic pressure, the length of the sample decreases about 2-3mm depends on the magnitude of hydrostatic pressure and the amount of the clearance between sample and SIHPT die.



**Fig. 4** The lines scribed on SIHPT samples in order to trace a rotation angle.

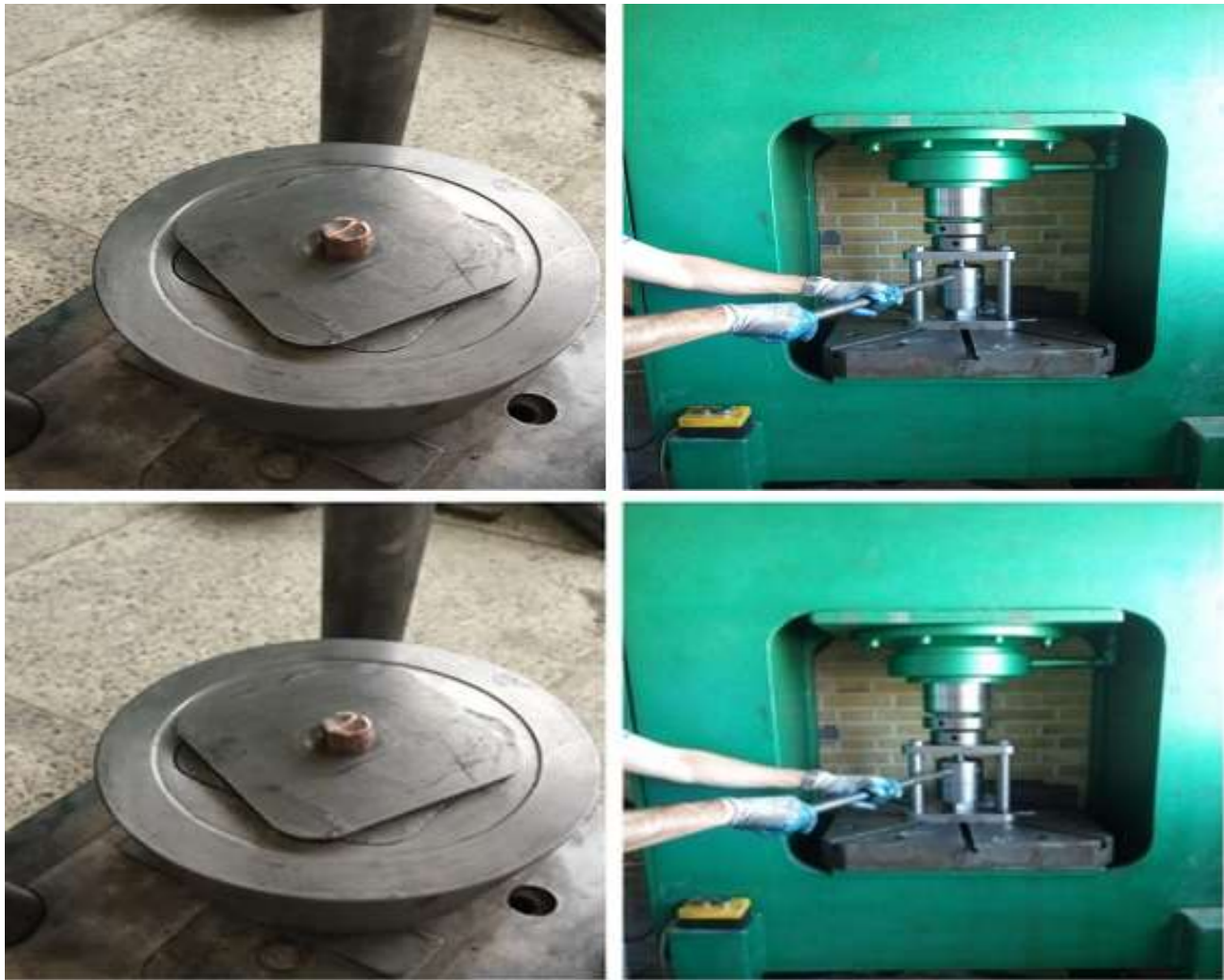


**Fig. 5** A scribed sample inside SIHPT die (left), whole SIHPT setup (right).

After the rotation of the sample to about e.g.  $\frac{1}{4}$  revolutions (“Fig. 5 (right)”), it anticipated that the extension of the scribed line in a rotating side to also rotate to about 90 degrees.

#### 4.3. Finite Element Modelling

In this study 3D FEM simulation of the SIHPT process has been conducted. Here, the specimen is modelled as a deformable member, however, the die is considered as a rigid body. A linear C3D8R element type from an explicit library of the Abaqus software is chosen for the meshing of the specimen. C3D8R is an eight-node brick element with reduced integration. Thanks to reduced integration characteristic of the element, not only the locking phenomenon are eliminated; but also the computation time is reduced considerably. The latter is vital in modelling of SIHPT process. About the precision, this element is preferred to full integrated element (C3D8) in plasticity and problems that involve high strains. The integration point of the C3D8R element is located in the middle of the element and then stress

and strain values are most accurate in the integration points. Hence, small elements are required to capture a stress concentration at the weak points of the model. Hourglassing is the main issue in using this element. To ensure that Hourglassing will not affect the results, in this study the Hourglass control is set in enhanced mode. High concentrated stress and strains caused element distortion during the modelling. To escape these exhausting interruptions, ALE adaptive remeshing technique was used in the simulations. However, despite all measures, still it is seen that there are some elements with very high undesired strains. By many trials and errors, it was found that by changing incremental time from step module this problem is fixed. The R3D4 element type is employed for meshing rigid bodies. The specimen and rigid bodies were constituted from 23328 and 17888 elements, respectively. The general contact property is defined for the contact between the cylindrical surface and also sample tips with die internal walls as well as the interference surfaces of the die. Penalty method was used for tangential behaviour in

interaction properties. The material type was pure copper which its behaviour was estimated by  $\sigma=340\varepsilon^{0.25}$  [11]. In this relation,  $\sigma$  stands for flow stress and  $\varepsilon$  shows the plastic strain. As discussed earlier, a friction ratio for using in modelling was obtained experimentally. The measurements showed that the friction ratio for this system is 0.22 that is valid for all pressures higher than 0.8 GPa. This value is used in all contact surfaces between the specimen and steel die. The angular rotation of the anvils was set in 1 rev/min that is several times higher than the angular speed of real experiment [17]. In practice due to the high heat output, it is not feasible to use higher speeds. However, as it is experimentally proved by Gurau et al [20], if the heat output can be controlled, it is possible to use angular speeds higher than 100 rev/min in HPT process. This means that if the effect of heat is neglectable, then the stress values calculated on elements do not differ by changing speed [21]. In the current modelling problem, the heat was not included in the modelling and then using higher speeds in simulations would not affect the results.

## 5 RESULTS AND DISCUSSION

### 5.1. Finite Element Analysis

At the first stage of the SIHPT process, a pressure was set on a sample using a hydraulic machine. But, the analysis shows that a really induced hydrostatic pressure on a sample due to the pressure of hydraulic machine is normally less than the applied pressure. In addition, the induced pressure on a sample is not uniform throughout the length of the sample. The main parameter which controls the magnitude of really induced pressure on a sample and the uniformity of the produced pressure throughout the length of a sample is the corner radius of the Steppers. Under the huge pressure the material fills any clearance between the sample and cavity; it also flows out to the gap between fixed and rotating anvils. This causes a loss in length of a sample which can considerably affect the real pressure on a sample. The other important influencing factor is friction forces. The friction forces may cause the difference between the pressures in the top and bottom of the sample. Figure 6 indicates the variation in the value of hydrostatic pressure along the length of the specimen (Z). As it is clear from "Fig. 6", the amount of hydrostatic pressure is considerably higher at the interface of rotating Steppers and 20% pressure changes can be observed along the length of the specimen. The parameter of corner radius controls the amount of material flow and consequently, affects the really produced hydrostatic pressure in a specimen. It means that without a precise design of Steppers' corner radius, using high pressure values on a specimen does not guarantee the production

of the same pressure entire the length of the specimen. Figure 7 shows the time history curves of real hydrostatic pressure in a specimen for 4 different corner radiuses of the steppers. In all these simulations, the applied hydrostatic pressure on a specimen was 1.5GPa. As can be seen in "Fig. 7", the maximum achieved hydrostatic pressure is considerably differing with a change in the amount of corner radius. According to this figure as the corner radius increases, the introduced hydrostatic pressure increases as well. According to "Fig. 7", there is a jump in introduced pressure by changing corner radius from 0.5 to 1mm. By increasing pressure, the specimen starts plastic deformation and flows between rotating Steppers. The material firstly starts to fill the volume at corner radius, afterwards by much increasing in pressure and in the case of gap presence between sliding steppers, the material flows out into the gap and produces a flash. Consequently, the corner radius of the steppers determines the regime of the process and the magnitude of the real hydrostatic pressure at the specimen. When the corner radius is greater than 1mm, the material does not fill the gap between rotating Steppers and two sliding steppers can touch each other without restraining by any flash material.

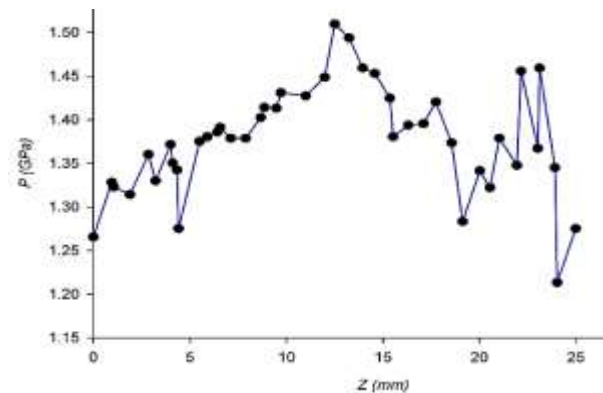


Fig. 6 The results of the FEM simulation for the change of real pressure along the length of the sample (Z) for 1.5GPa applied pressure.

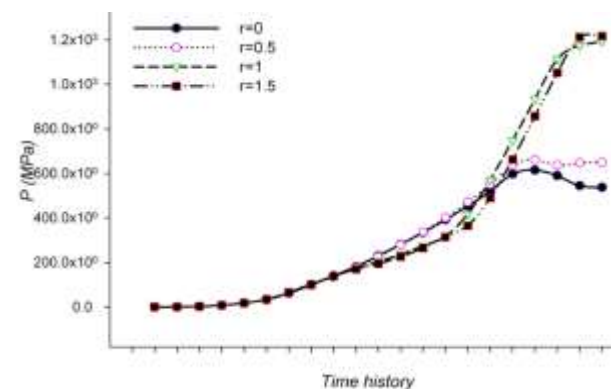


Fig. 7 The FEM results of the relation between Steppers' corner radius and a real pressure on a sample.

Figure 8 shows vMises type stress distribution throughout the work specimen for 1.5GPa applied pressure and 1mm corner radius.

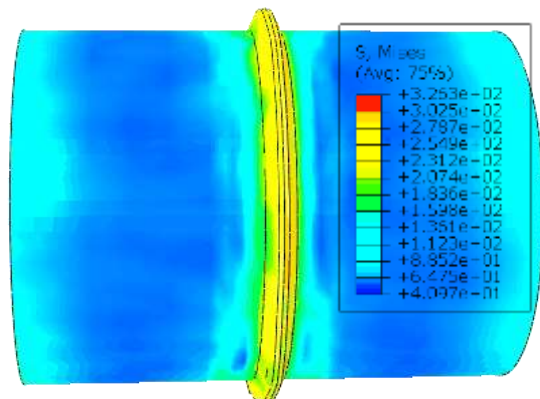


Fig. 8 vMises type stress distribution throughout the work specimen for 1.5GPa applied pressure and a 1mm corner radius.

As it can be seen no flash produces in this state and a zone near the interface endures the maximum stress values. As a conclusion, according to finite element

analysis, really introduced pressure on a sample is not necessarily equal with applied load and it depends on many parameters such as distance from the top of the sample and the corner radius of the steppers. In this study, according to the discussion above, 1mm corner radius is chosen for fabrication of Steppers. Because, it was found that this amount of corner radius introduces the highest hydrostatic pressure and at the same time the minimum material deformation occurs.

### 5.2. Experiments for Slippage

Different samples with about 28mm length are prepared. The length of samples after the application of pressure was about 25mm. When scribing lines on raw samples, it was found that after the application of hydrostatic pressure, the line hardly can be distinguished, however when scribing the lines on samples after first SIHPT revolution, scribed lines can easily be distinguished after experiments. Here, the lowest contact length of a sample considered to be 5mm for the hydraulic pressure of about 0.8GPa. Under this load, samples are rotated to about 90, 180, 360 and 720 degrees in different experiments. Afterwards, the angle of rotation of the scribed lines is measured (“Fig. 9”).

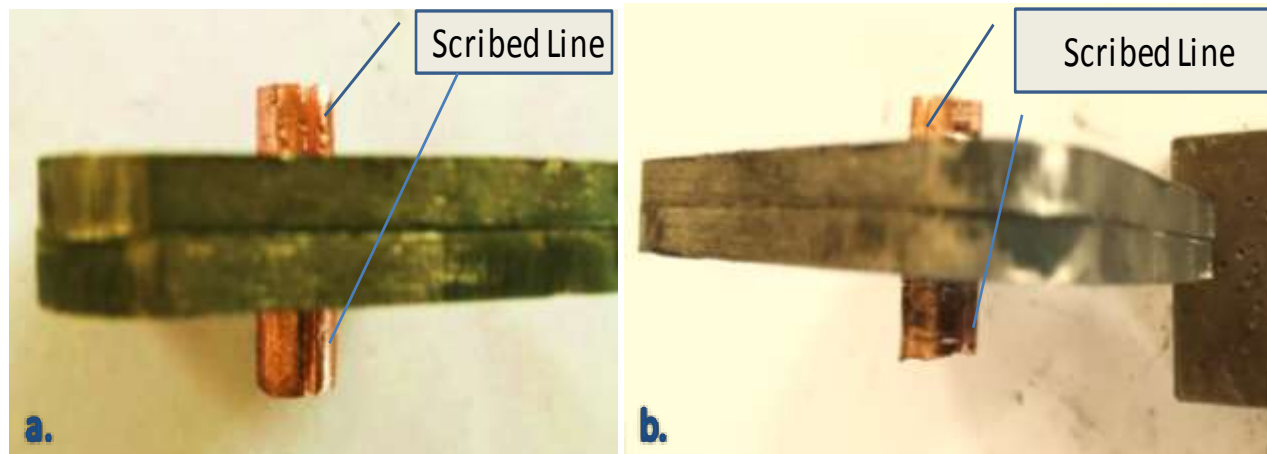


Fig. 9 (a): scribed line before rotation in IHPT rig and (b): scribed line after 90-degree rotation in IHPT rig.

It was found that for 5mm contact length, the maximum 22% slippage can occur. However, by increasing the length of contact to about 10mm, the slippage reduces to a maximum of about 8%. The results of measurements for slippage have been illustrated in “Fig. 10”. As it is obvious from “Fig. 10”, there is no considerable dependence between the slippage percentage and SIHPT rotation. But the slippage between the sample and die is decreased by increasing lower contact length (L) which is rational according to “Eq. 4”. The other parameter which is considered in this study was the rotation speed during SIHPT process. The speed of rotation in SIHPT process is relatively low in comparison with the conventional HPT process. This is because the heat

production is more important in SIHPT process than conventional HPT. The results of the experiments revealed that increasing the rotation speed noticeably increases the slippage (“Fig. 11”).

However, in higher pressures this effect fade away gradually and in 1.5GPa hydrostatic pressure it can be said that the rotation speed has no remarkable effect on the amount of slippage. As it is shown in “Fig. 12(a)”, in pressures higher than 1.5GPa, the sample surface completely sticks on a die wall, where a relatively thick layer of the sample remains on steppers internal surface after dislodge of the sample from the steppers. However, in lower pressures only a very thin layer of the copper sample remains on steppers’ wall (“Fig. 12(b)”).

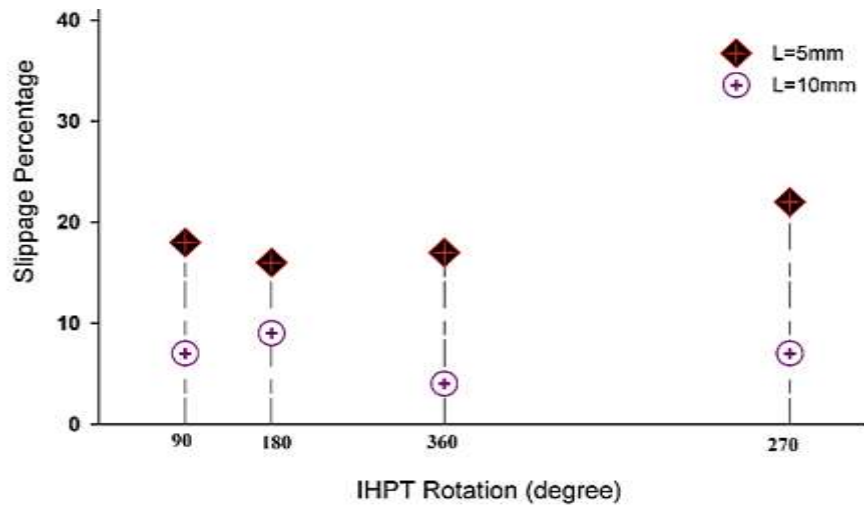


Fig. 10 variation of the slippage by increasing in IHPT rotation; the rotation speed and applied pressure were 2rpm and 0.8GPa, respectively.

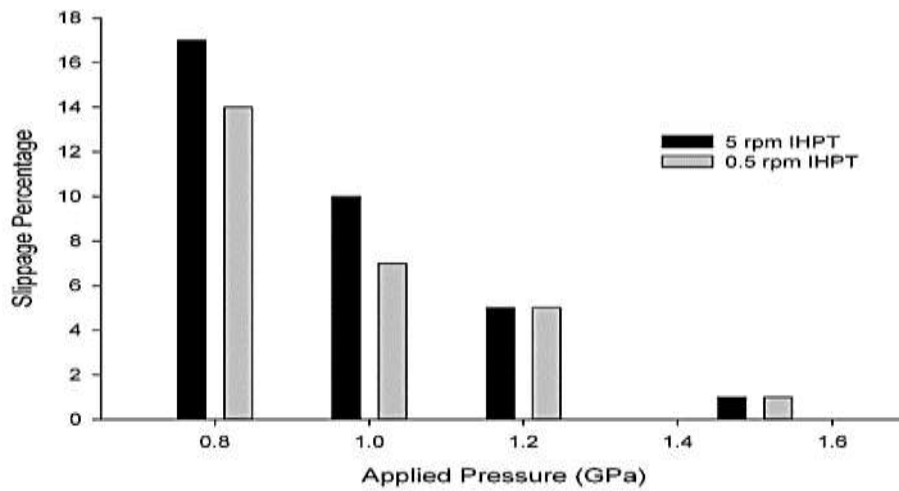


Fig. 11 Dependence of slippage to rotation speed and applied load.

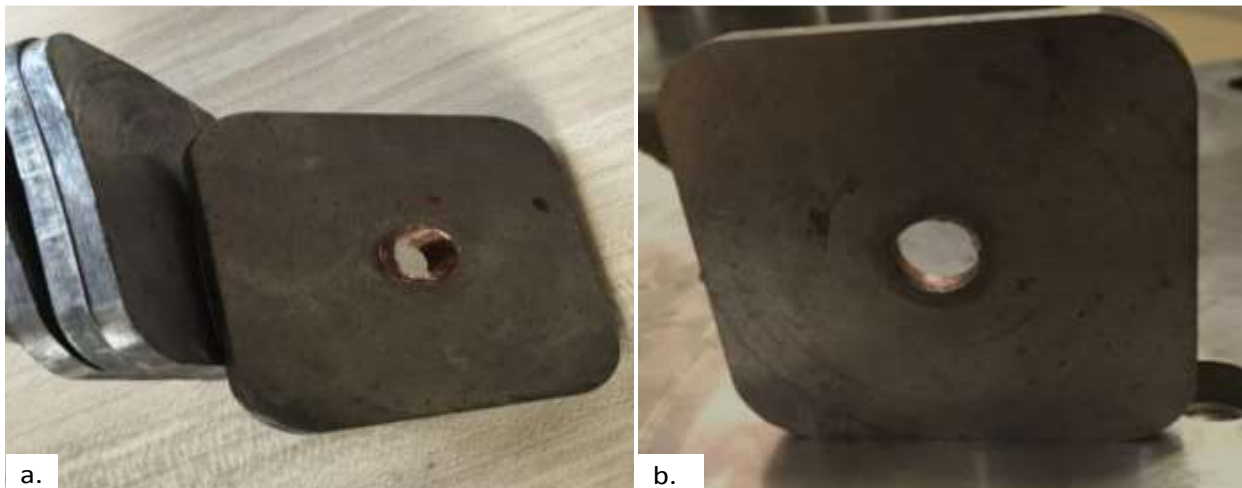


Fig. 12 Remained Layer of the copper sample on Anvil wall: (a): 1.5GPa and (b): 0.8 GPa.



---

## 6 CONCLUSION

---

SIHPT is a conventional HPT based method of processing relatively long materials to produce nanostructured microstructure. This study was dedicated to study different design parameters of Steppers which play important role in SIHPT process. These parameters include corner radius, Steppers's thickness and slippage phenomenon. Here, FEM analysis is done in order to obtain an optimal value for the corner radius. Using FEM, the distribution of induced hydrostatic pressure through the length of the sample was also studied. Afterwards, the amounts of slippage for different conditions are measured, experimentally. The following results are achieved:

- The real hydrostatic pressure on a sample is considerably less than actually applied pressure. In addition, the distribution of applied pressure throughout the sample length is not uniform and has about 20% variation.
- It was found that the corner radius of the steppers has a substantial effect on the magnitude of the really produced hydrostatic pressure. Finite element study showed that for the dimensions and materials of the current study, 1mm is the best choice for corner radius of the steppers which leads to the highest real pressure on a sample
- During SIHPT process, there is substantial slippage between copper sample and die wall in pressures lower than 1 GPa. It was found that the amount of slippage decreases sizeably by increasing one/both of the applied load and contact length (L) of the sample inside fixed steppers. Furthermore, it was shown that the slippage has less dependence on rotation speed in high pressures.

---

## REFERENCES

---

- [1] Valiev, R., Kuznetsov, O., Musalimov, R. S., and Tsenev, N., Low-Temperature Superplasticity of Metallic Materials, Soviet Physics Doklady, 1988, pp. 626.
- [2] Zhilyaev, A. P., Langdon, T. G., Using High-Pressure Torsion for Metal Processing: Fundamentals and Applications. Progress in Materials Science, Vol. 53, 2008, pp. 893-979.
- [3] Polakowski, N. H., Ripling, E. J., Strength and Structure of Engineering Materials. 1rd ed, Prentice Hall, 1966, pp. 346-348, 978-0138517908.
- [4] Levitas, V. I., Zarechnyy, O. M., Numerical Study of Stress and plastic Strain Evolution Under Compression and Shear of a Sample in a Rotational Anvil Cell, High Pressure Research, Vol. 30, 2010, pp. 653-691.
- [5] Kim, H. S., Finite Element Analysis of High Pressure Torsion Processing, Journal of Materials Processing Technology Vol. 113, No. 21, 2001, pp. 617-618.
- [6] Lee, D. J., Yoon, E. Y., Lee, S. H., Kang, S. Y., and Kim, H. S., Finite Element Analysis for Compression Behavior of High Pressure Torsion Processing, Rev Adv Mater Sci, Vol. 31, No. 30, 2012, pp. 25-30.
- [7] Wang, W., Song, Y., Gao, D., Yoon, E. Y., Lee, D. J., and Lee, C. S., et al, Analysis of Stress States in Compression Stage of High Pressure Torsion Using Slab Analysis Method and Finite Element Method, Metals and Materials International, Vol. 19, No. 7, 2013, pp. 1021-1022.
- [8] Zhilyaev, A, Oh-Ishi, K., Langdon, T., and McNelley, T., Microstructural Evolution in Commercial Purity Aluminum During High-Pressure Torsion, Materials Science and Engineering: A, Vol. 410, No. 80, 2005, pp. 277-278.
- [9] Draï, A., Aour, B., Analysis of Plastic Deformation Behavior of HDPE During High Pressure Torsion Process, Engineering Structures, Vol. 46, No. 93, 2013, pp. 87-93.
- [10] Verleysen, P., Van den Abeele, F., and Degrieck, J., Numerical Simulation of HPT Processing, IOP Conference Series: Materials Science and Engineering: IOP Publishing, 2014, pp. 012043.
- [11] Figueiredo, R. B., Cetlin, P. R., and Langdon, T. G., Using Finite Element Modeling to Examine the Flow Processes in Quasi-Constrained High-Pressure Torsion, Materials Science and Engineering: A, Vol. 528, No. 204, 2011, pp. 8198-8198.
- [12] Song, Y., Wang, W., Gao, D., Yoon, E., Lee, D., and Kim, H., Finite Element Analysis of the Effect of Friction in High Pressure Torsion, Metals and Materials International, Vol. 20, No. 50, 2014, pp. 445-446.
- [13] Figueiredo, R. B., Pereira, P. H. R., Aguilar, M. T. P., Cetlin, P. R., and Langdon, T. G., Using Finite Element Modeling to Examine the Temperature Distribution in Quasi-Constrained High-Pressure Torsion, Acta Materialia, Vol. 60, No. 8, 2012, pp. 3190-3191.
- [14] Jahedi, M., Knezevic, M., and Paydar, M. H., High-Pressure Double Torsion as a Severe Plastic Deformation Process: Experimental Procedure and Finite Element Modelling, Journal of Materials Engineering and Performance, Vol. 24, No. 82, 2015, pp. 1471-1472.
- [15] Yoon, S. C., Horita, Z., and Kim, H. S., Finite Element Analysis of Plastic Deformation Behavior During High Pressure Torsion Processing, Journal of Materials Processing Technology, Vol. 201, No. 6, 2008, pp. 32-33.
- [16] Halloumi, A., Busquet, M., and Descartes, S., Parametric Study of Unconstrained High-Pressure Torsion-Finite Element Analysis, IOP Conference Series: Materials Science and Engineering: IOP Publishing, 2014, pp. 012036.
- [17] Hohenwarter, A., Incremental High Pressure Torsion as a Novel Severe Plastic Deformation Process: Processing Features and Application to Copper, Materials Science

- and Engineering: A, Vol. 626, No. 5, 2015, pp. 80-81.
- [18] Eskandarzade, M., Masoumi, A., Faraji, G., Mohammadpour, M., and Yan, X. S., A New Designed Incremental High Pressure Torsion Process for Producing Long Nanostructured Rod Samples, *Journal of Alloys and Compounds*, Vol. 695, No. 46, 2017, pp. 1539-1540.
- [19] Sharifi Miavaghi, A., Kangarlou, H., and Eskandarzade, M., Comparison Between Frictional Behavior of the Soft and Brittle Materials at Different Contact Pressures, *Lebanese Science Journal*, Vol. 18, No. 1, 2017, pp. 98.
- [20] Gurău, G., Gurău, C., Potecașu, O., Alexandru, P., and Bujoreanu, L. G., Novel High-Speed High Pressure Torsion Technology for Obtaining Fe-Mn-Si-Cr Shape Memory Alloy Active Elements, *Journal of Materials Engineering and Performance*, Vol. 23, No. 402, 2014, pp. 2396-2397.
- [21] Chung, S. W., Kim, W. J., Kohzu, M., and Higashi, K., The Effect of Ram Speed on Mechanical and Thermal Properties in ECAE Process Simulation, *Materials Transactions*, Vol. 44, No. 80, 2003, pp. 973.